

1 **Asymmetry of fibrillar plaque burden in amyloid mouse models**

2

3 **Christian Sacher¹, Tanja Blume^{1,2}, Leonie Beyer¹, Gloria Biechele¹, Julia**
4 **Sauerbeck¹, Florian Eckenweber¹, Maximilian Deussing¹, Carola Focke¹, Samira**
5 **Parhizkar³, Simon Lindner¹, Franz-Josef Gildehaus¹, Barbara von Ungern-**
6 **Sternberg¹, Karlheinz Baumann⁴, Sabina Tahirovic², Gernot Kleinberger^{3,5,6},**
7 **Michael Willem³, Christian Haass^{2,3,5}, Peter Bartenstein¹, Paul Cumming^{7,8}, Axel**
8 **Rominger^{1,7}, Jochen Herms^{2,5,9}, Matthias Brendel^{1,5}**

9 ¹Dept. of Nuclear Medicine, University Hospital of Munich, LMU Munich, Munich Germany

10 ²DZNE - German Center for Neurodegenerative Diseases, Munich, Germany

11 ³Chair of Metabolic Biochemistry, Biomedical Center (BMC), Faculty of Medicine, LMU Munich,
12 Munich, Germany

13 ⁴Roche Pharma Research and Early Development, F. Hoffmann-La Roche Ltd., Basel,
14 Switzerland

15 ⁵Munich Cluster for Systems Neurology (SyNergy), Munich, Germany

16 ⁶ISAR Bioscience GmbH, Planegg, Germany

17 ⁷Department of Nuclear Medicine, Inselspital, University Hospital Bern, Bern, Switzerland

18 ⁸School of Psychology and Counselling and IHBI, Queensland University of Technology,
19 Brisbane, Australia

20 ⁹Center of Neuropathology and Prion Research, University of Munich, Munich Germany

21

22 **Abbreviated title:** A β plaque asymmetry in mice

23 **Corresponding author:** Dr. Matthias Brendel; Department of Nuclear Medicine, University of
24 Munich; Marchioninistraße 15, 81377 Munich, Germany; Phone:+49(0)89440074650,
25 Fax:+49(0)89440077646; E-Mail:matthias.brendel@med.uni-muenchen.de

26

27 **First author:**

28 Christian Sacher (medical student); Department of Nuclear Medicine; LMU Munich, Germany;
29 Phone:+49(0)1623878661; E-Mail:christian.sacher@med.uni-muenchen.de

30

31 **Word count: 5000**

32

1 **ABSTRACT**

2 **Objective:** Asymmetries of amyloid- β ($A\beta$) burden, are well-known in Alzheimer's
3 disease (AD), but did not receive attention in $A\beta$ mouse models of AD. Therefore, we
4 investigated $A\beta$ -asymmetries in $A\beta$ mouse models examined by $A\beta$ - small animal
5 positron-emission-tomography (PET) and tested if such asymmetries have an
6 association with microglial activation. **Methods:** 523 cross-sectional $A\beta$ -PET scans of
7 five different $A\beta$ mouse models (APP/PS1, PS2APP, APP-SL70, *App*^{NL-G-F} and APPswe)
8 were analyzed together with 136 18kDa translocator protein (TSPO)-PET scans for
9 microglial activation. The asymmetry index (AI) was calculated between tracer uptake in
10 both hemispheres. AIs of $A\beta$ -PET were analyzed in correlation with TSPO-PET AIs.
11 Extrapolated required sample sizes were compared between analyses of single and
12 combined hemispheres. **Results:** Relevant asymmetries of $A\beta$ deposition were identified
13 in $\geq 30\%$ of all investigated mice. There was a significant correlation between AIs of $A\beta$ -
14 PET and TSPO-PET in four investigated $A\beta$ mouse models (APP/PS1: $R=0.593$,
15 $P=0.001$; PS2APP: $R=0.485$, $P=0.019$; APP-SL70: $R=0.410$, $P=0.037$; *App*^{NL-G-F}:
16 $R=0.385$, $P=0.002$). Asymmetry was associated with higher variance of tracer uptake in
17 single hemispheres, leading to higher required sample sizes. **Conclusions:** Asymmetry
18 of fibrillar plaque neuropathology occurs frequently in $A\beta$ mouse models and acts as a
19 potential confounder in experimental designs. Concomitant asymmetry of microglial
20 activation indicates a neuroinflammatory component to hemispheric predominance of
21 fibrillary amyloidosis.

22

23 **Key words:** asymmetry, amyloid, microglia, mouse models

24

1 INTRODUCTION

2 Alzheimer disease (AD) is the most frequent neurodegenerative disease, with
3 burgeoning incidence rates due to the rising life expectancy in most of the world (1). The
4 neuropathology of AD is histologically characterized by the triad of accumulation of
5 amyloid- β peptide (A β) as extracellular plaques, fibrillary tau aggregates within neurons,
6 and the activation of multiple neuroinflammatory pathways, which is mediated by
7 activated microglia expressing high levels of the marker 18-kDa translocator protein
8 (TSPO) (2). Animal models that accurately reflect this complex pathology are
9 indispensable for contemporary preclinical research into the molecular mechanisms of
10 AD. In this context, a range of different overexpressing and knock-in A β mouse models
11 have been established for molecular imaging with positron emission tomography (PET).
12 In recent PET studies, increased binding of the A β tracer ^{18}F -florbetaben (^{18}F -FBB) and
13 the TSPO tracer ^{18}F -GE-180 were firmly established by longitudinal *in vivo* quantification
14 of cerebral amyloidosis and microglial activation in various A β mouse models of AD (3-
15 5). In humans, an asymmetric spatial distribution of neuropathological AD hallmarks is
16 frequently discovered by PET studies *in vivo* (6-8). A recent human PET study has
17 already shown that asymmetric spatial distributions of A β plaques are positively
18 correlated with ipsilateral neurodegeneration (8). However, no study has hitherto
19 investigated systematically the asymmetry in A β mouse models of AD. While a large
20 scaled investigation of this phenomenon by histopathological investigations would be of
21 high economic effort and difficult in terms of standardization, *in vivo* PET imaging
22 methods should afford the means to compare readily the A β plaque burden in both
23 hemispheres of individual animals.

24 Given this background, our aim was to investigate the occurrence of asymmetric
25 fibrillar A β deposition in the well-established A β mouse models APP/PS1, PS2APP,
26 APP-SL70, *App*^{NL-G-F} and APP^{swe}. Using a large series of historical ^{18}F -FBB A β -PET

1 recordings, we tested for asymmetric A β deposition, while considering age as a
2 predictive variable. We also made sample size estimations for detecting asymmetric A β ,
3 and tested the hypothesis that A β asymmetry is associated with ipsilateral microglial
4 activation as assessed by ¹⁸F-GE-180 TSPO-PET.

5

6 **MATERIAL AND METHODS**

7 **Experimental Design**

8 All experiments were performed in compliance with the National Guidelines for
9 Animal Protection, Germany and with the approval of the regional animal committee
10 (Regierung Oberbayern) and were overseen by a veterinarian. Animals were housed in
11 a temperature- and humidity-controlled environment with 12h light-dark cycle, with free
12 access to food (Sniff, Soest, Germany) and water. A detailed overview of the
13 investigated mouse cohorts is given in Supplemental Table 1. All PET raw data
14 originated from previous in-house studies (cited below) conducted on the same Inveon
15 small animal PET under identical acquisition parameters. 87% of the mice investigated
16 were female. APP/PS1 and APP^{swe} comprised only female mice, whereas PS2APP,
17 APP-SL70, and *App*^{NL-G-F} included both sexes. All raw data were reprocessed to
18 guarantee optimal agreement of spatial and radioactivity normalization. Either
19 descriptive datasets or control groups of therapy/ genotype studies were included. From
20 each investigated mouse, the degree of asymmetry in A β -PET and TSPO-PET was
21 assessed by volume-of-interest based quantification in both cerebral hemispheres.

22

23 **Animal Models**

24 *APP/PS1 (APPPS1-21)*: This transgenic mouse model was generated on a C57BL/
25 6J genetic background that coexpresses KM670/671NL mutated amyloid precursor
26 protein and L166P mutated presenilin 1 under the control of a neuron-specific Thy1

1 promoter. Cerebral amyloidosis in this model starts at 6–8 weeks of age (9). Historical
2 ¹⁸F-FBB data from 41 scans of APP/PS1 mice imaged at four different ages (3, 6, 9 and
3 12 months) were reprocessed (10). 27 contemporaneous ¹⁸F-GE-180 scans were
4 available.

5 *PS2APP (APP^{swe}/PS2)*: The transgenic B6.PS2APP (line B6.152H) is homozygous
6 both for human presenilin (PS) 2, the N141I mutation, and the human amyloid precursor
7 protein (APP) K670N/M671L mutation (11). Homozygous B6.PS2APP mice show first
8 appearance of plaques in the cerebral cortex and hippocampus at 5–6 months of age
9 (12). Historical ¹⁸F-FBB data from 147 scans of PS2APP mice imaged at four different
10 age ranges (6–8, 9–10, 11–14 and 15–17 months) were reprocessed (13,14). 23
11 contemporaneous ¹⁸F-GE-180 scans from these mice were likewise reprocessed by
12 standard methods.

13 *APP-SL70*: The PS1 knock-in line was generated by introducing two-point mutations
14 in the wild-type mouse PSEN1, corresponding to the mutations M233T and L235P. The
15 APP751SL mouse overexpresses human APP751 carrying the London (V717I) and
16 Swedish (K670N/M671L) mutations under the control of the Thy1 promoter. Aβ deposits
17 appear as early as 2.5 months of age in these mice (15). Historical ¹⁸F-FBB data from
18 208 scans of APP-SL70 mice imaged at four different ages (4–6, 7–9, 10–12 and 13–15
19 months), deriving from a descriptive observational study (16), along with control scans
20 from an as yet unpublished therapy study were reprocessed. 26 contemporaneous ¹⁸F-
21 GE-180 scans were available in this group.

22 *App^{NL-G-F}(App^{NL-G-F/NL-G-F})*: The knock-in mouse model *App^{NL-G-F}* carries a mutant APP
23 gene encoding the humanized Aβ sequence (G601R, F606Y, and R609H) with three
24 pathogenic mutations, namely Swedish (KM595/596NL), Beyreuther/Iberian (I641F), and
25 Arctic (E618G). Homozygous *App^{NL-G-F}* mice progressively exhibit widespread Aβ
26 accumulation from two months of age (17,18). Historical ¹⁸F-FBB data from 55 scans of

1 homozygotic *App*^{NL-G-F} mice imaged at four different ages (2.5, 5.0, 7.5 and 10 months)
2 were reprocessed (3). 55 contemporaneous ¹⁸F-GE-180 scans were available in this
3 data set.

4 *APP*^{swe}: Transgenic mice overexpressing human APP with the Swedish double
5 mutation (K670N, M671L) driven by the mouse Thy1.2 promoter were generated as
6 described earlier (11). Mice heterozygous for the transgene begin accumulating β-
7 amyloid at approximately nine months of age and develop β-amyloid plaques at twelve
8 months of age, mainly in the cortical mantle. Historical ¹⁸F-FBB data from 72 scans of
9 APP^{swe} mice imaged at three different age ranges (9–12, 13–16 and 17–20 months)
10 were reanalyzed (19,20). Contemporaneous ¹⁸F-GE-180 scans were not available for
11 these mice.

12 *C57Bl/6*: Historical and unpublished ¹⁸F-FBB data from 27 scans of C57Bl/6 mice
13 (WT) were reprocessed and served as control material (age: 2.5-16 months).

14

15 **PET Imaging**

16 *PET Data Acquisition, Reconstruction and Post-Processing*: For all PET procedures,
17 radiochemistry, data acquisition, and image pre-processing were conducted according to
18 an established, standardized protocol (4,21). In brief, ¹⁸F-FBB Aβ PET recordings
19 (average dose: 11.4±2.0 MBq) with an emission window of 30–60 min after injection
20 were obtained to measure fibrillar cerebral amyloidosis. ¹⁸F-GE-180 TSPO PET
21 recordings (average dose: 11.1±2.0 MBq) with an emission window of 60–90 min after
22 injection were performed for assessment of cerebral TSPO expression. Anesthesia was
23 maintained from just before tracer injection to the end of the imaging time window.

24 *PET Image Analysis*: We performed all analyses using PMOD (version 3.5; PMOD
25 technologies). Normalization of emission images to standardized uptake value ratio
26 (SUVR) images was performed using previously validated white matter (WM) reference

1 regions for transgenic amyloid mouse models (APP/PS1, PS2APP, APP-SL70 and
2 APP^{swe}) (4,21). For the knock-in mouse line *App*^{NL-G-F}, the mesencephalic
3 periaqueductal gray (PAG) was used as reference region, as recently published (3). Two
4 bilateral telencephalic volumes of interest (VOIs) (containing cortex and hippocampus)
5 comprising 50 mm³ each, were employed for calculation of SUVR_{Forebrain/WM} or
6 SUVR_{Forebrain/PAG}. For each scan, the hemispheric asymmetry index (AI) was calculated
7 for ¹⁸F-FBB or ¹⁸F-GE-180 scans using the formula:

$$8 \quad \text{AI}[\%] = 200 \times (R - L) / (R + L)$$

9 .

10 **Statistical Analysis**

11 95% and 99% confidence intervals (CI) of ¹⁸F-FBB AIs in normal C57BL/6 mice
12 were calculated. A β mouse model ¹⁸F-FBB scans were judged as asymmetric when they
13 exceeded the 95%-CI (moderate asymmetry) or the 99%-CI (strong asymmetry) of
14 C57BL/6 mice. Significant ¹⁸F-FBB |AIs| (absolute magnitude) were correlated with age
15 for each A β mouse model to evaluate age-dependency of asymmetric plaque
16 distribution. For each A β mouse model, age-independent lateralized plaque distributions
17 were compared by a Chi-square test to test for left or right predominance of A β
18 deposition. Frequency of strong asymmetries were calculated in groups of comparable
19 age for A β mouse models and correlated with coefficients of variance (CoV) of SUVR in
20 the same groups of mice. Pearson's coefficients of correlation (*R*) were calculated for
21 the latter analyses and for correlation analyses between ¹⁸F-FBB AIs and age as well as
22 between ¹⁸F-FBB AIs and ¹⁸F-GE-180 AIs. Hypothetical 2-sided t-test of independent
23 measures were performed in order to perform sample sizes calculations in comparison
24 of SUVR in single hemispheres and in combined hemispheres using G*Power (V3.1.9.2,
25 Kiel, Germany). We used a given 5% therapy effect on SUVR at a power (1- β) of 0.80
26 and type one error of $\alpha=0.05$. A *P*-value of less than 0.05 was considered to be

1 significant for rejection of the null hypothesis. SPSS 25 statistics (IBM Deutschland
2 GmbH, Ehningen, Germany) was used for all statistical tests.

3

4 **RESULTS**

5 **Asymmetric Plaque Distribution is Frequent in A β Mouse Models**

6 First, we defined an asymmetry threshold based on PET measurements in WT
7 mice to establish real A β asymmetry, without bias in the spatial normalization or by
8 physiological variability in tracer uptake. The 95%-CI of ¹⁸F-FBB AIs in C57BL/6 mice
9 was -3.6% (right lateralization) to 3.6% (left lateralization) and defined the threshold for
10 moderate A β asymmetry. The 99%-CI of ¹⁸F-FBB AIs in C57BL/6 was -4.0% (right
11 lateralization) to 4.5% (left lateralization) and defined the threshold for strong A β
12 asymmetry. Using these thresholds, 40% (L=21%; R=19%; 95%-CI) of all amyloid
13 accumulating mice showed moderate asymmetry and 30% (L=14%; R=16%; 99%-CI)
14 showed strong asymmetry of ¹⁸F-FBB forebrain uptake (Figure 1). There was no
15 significant hemispheric predominance across the whole cohort of different A β mouse
16 models. A detailed overview is provided in Supplemental Table 1.

17 Highest frequency of moderate A β -PET asymmetry was observed in PS2APP
18 and *App*^{NL-G-F} mice (49% each). Strong A β -PET asymmetry was most frequently
19 observed in PS2APP and APP/PS1 mice (37% each). Lowest frequency of A β -PET
20 asymmetry was present in APP^{swe} mice, in which 32% of scans indicated moderate and
21 24% showed strong asymmetry. A significant left-hemispheric predominance of A β
22 deposition was detected in the PS2APP mice ($\chi^2=4.7$; $P=0.030$; Chi-square test),
23 whereas a significant right-hemispheric predominance of A β deposition was seen in
24 APP^{swe} mice ($\chi^2=15$; $P=0.0001$; Chi-square test). There was no significant association
25 between age and asymmetric A β distribution in any A β mouse model (Figure 2). In
26 summary, asymmetry of plaque burden was frequently observed in all studied A β mouse

1 models, but with different magnitudes and side predilections.

2

3 **Asymmetric Plaque Burden Impacts the Sufficient Sample Sizes in Preclinical** 4 **Trials**

5 Given the observed asymmetries in all A β mouse models studied, we
6 hypothesized that measures in single hemispheres (as are typically examined by
7 histological methods) would suffer from higher variance, subsequently leading to higher
8 required sample sizes in preclinical trials when compared to combined measures of both
9 hemispheres, as are obtained by PET. CoV were positively associated with the
10 frequency of plaque burden asymmetry (99%-CI) in groups of comparable age in
11 different A β mouse models ($R=0.380$, $P=0.027$, Figure 3A). CoV by groups of
12 comparable age in the different A β mouse models were $4.3\pm 1.2\%$ for separate
13 measures of left and right hemispheres and significantly lower for the combined
14 quantification of both hemispheres ($3.9\pm 1.2\%$; $P = \text{left vs. both: } 0.0003/ \text{right vs. both:}$
15 0.0007 ; paired t -test). Calculated sample sizes for detection of a 5% therapy effect on
16 SUVR at a power ($1-\beta$) of 0.80 and type one error of $\alpha=0.05$ were $n=14.1$ for separate
17 measures for the left hemisphere, $n=13.9$ for separate measures of the right
18 hemisphere, and $n=11.9$ for combined quantification of both hemispheres
19 ($P=0.0020/0.0016$; paired t -test). Required sample sizes as a function of power were
20 consistently higher for calculation with left (Figure 3B) and right (Figure 3C) hemispheric
21 values when compared to combined quantification of both hemispheres. The average
22 reductions of required sample sizes for combined quantification of both hemispheres
23 were 2.1 ± 0.6 (vs. left) and 1.8 ± 0.5 (vs. right). These results indicate that asymmetry of
24 plaque burden in A β mouse models considerably increases required sample sizes when
25 hemispheres are analyzed separately.

26

1 **Asymmetric Plaque Burden is Associated with Ipsilateral Glial Activation**

2 Several studies have revealed associations between amyloid deposition and
3 microglial activation in A β mouse models (3,4,16). However, it has not hitherto been
4 investigated if microglial activation follows any asymmetry of plaque burden, or if the
5 microgliosis is globally distributed. Hence, we made use of contemporaneous TSPO-
6 PET data for correlation analysis with lateralization to A β -PET. Significant positive
7 associations between asymmetric A β deposition and ipsilateral lateralization of TSPO
8 expression were observed in all four A β mouse models (Figure 4). The magnitude of
9 correlation between asymmetric A β -PET and ipsilateralized TSPO-PET uptake was
10 similar among APP/PS1 ($R=0.593$; $P=0.001$; $n=27$; Pearson's correlation), PS2APP
11 ($R=0.485$; $P=0.019$; $n=23$; Pearson's correlation), APP-SL70 ($R=0.410$; $P=0.037$; $n=26$;
12 Pearson's correlation), and *App*^{NL-G-F} ($R=0.385$; $P=0.002$; $n=60$; Pearson's correlation)
13 mice. Taken together these results clearly indicate a spatial association between
14 asymmetric distribution of fibrillar A β plaques and ipsilateral microglial activation.

15

16 **DISCUSSION**

17 In contrast to human investigations on asymmetrical A β distribution in AD
18 (6,8,22), only scanty evidence is available for the presence of A β asymmetry in mouse
19 models (19,23). We present the first large-scale preclinical *in vivo* investigation of fibrillar
20 plaque burden asymmetry by standardized evaluation of PET data. With respect to
21 animal welfare guidelines, in particular reduction of animal numbers in accordance with
22 the 3R principle, we used scans from various earlier studies, this avoiding any
23 requirement for additional animal experiments to test our hypotheses.

24 First, we endeavored to establish a reasonable threshold of lateralized A β -PET
25 signal to exclude asymmetry findings driven by reasons other than A β pathology. To this

1 end, we used A β -PET data of C57BL/6 WT mice, as they are not known to manifest any
2 A β accumulation. Minor asymmetry of FBB tracer uptake in WT mice could be attributed
3 to factors such as differences in cerebral blood flow, differing hemispheric volumes, or
4 methodological issues such as lateralized spill-over of bone uptake, imperfect
5 attenuation correction, or bias in spatial normalization. Hence, we used the 95% and
6 99% CIs of ¹⁸F-FBB AIs in WT to discern moderate and strong asymmetry in the groups
7 of A β accumulating mice. By these criteria, 40% of all A β accumulating mice revealed
8 moderate asymmetry, and 30% showed strongly asymmetric A β deposition, but without
9 evidence for a general lateralization across all AD models. Nevertheless, two out of five
10 investigated amyloid models revealed significant lateralization of A β plaque distribution
11 to A β -PET. There was a significant left-hemispheric predominance of A β deposition in
12 PS2APP mice, but a significant right-hemispheric predominance in APP^{swe} mice. While
13 molecular explanations and causal mechanisms giving rise to this phenomenon are
14 presently unknown, we contend that this is a real phenomenon requiring special
15 consideration when comparing data from different A β mouse models of AD. For
16 example, a comparison of exclusively right hemisphere read-outs, as might be obtained
17 by histological analysis, between APP^{swe} and PS2APP could cause false negative
18 findings, and likewise for the left hemisphere. The highest frequency of asymmetry was
19 observed in A β models with a Presenilin mutation (PS2APP and APP/PS1), indicating
20 that involvement of this gene might increase the probability of asymmetric plaque
21 burden. Variable expression of APP mRNA across different PS2APP mice is already
22 postulated to be a key determinant of variance in individual A β deposition (12); therefore
23 we speculate that this phenomenon could likewise hold true for differences between
24 hemispheres.

25 By making sample size estimations, we established that the observed
26 asymmetries of fibrillar plaque burden are potentially relevant to the design of preclinical

1 trials. Importantly, the calculated sample sizes sufficient to detect relevant therapeutic
2 effects, which are comparable to those of earlier drug trials in these A β mouse models
3 (13,20), were significantly higher when only single hemispheres were analyzed, as
4 opposed to combined measurement of both hemispheres. As A β -PET and histology
5 markers for fibrillar A β were strongly intercorrelated in previous studies (10,19,24), we
6 assume that asymmetry effects on required sample sizes should also hold true for stand-
7 alone histological or biochemical analyses. This conjecture remains to be demonstrated,
8 since usual practice is to process one hemisphere for histology and one for
9 biochemistry. A β -PET findings at the terminal time-point could help to identify mice with
10 asymmetric plaque burden, which would allow consecutive adjustment of measures by
11 different modalities in separate hemispheres.

12 Next, we investigated whether asymmetric A β distributions occur in an age-
13 dependent manner. Our cross-sectional analysis of historical PET data did not indicate
14 any significant association of AI with age among the five A β mouse models. This is
15 consistent with our earlier longitudinal ¹⁸F-FBB-PET findings in APP^{swe}, where we
16 incidentally noticed that some animals showed consistently right-sided plaque
17 asymmetry between 13 and 20 months of age. More precisely, the magnitude of
18 asymmetry in SUVR increased with age, but with no temporal dependence of the AI *per*
19 *se* (19). In conclusion, A β asymmetries, when present, are established at the onset of
20 plaque deposition.

21 We suppose that there are hitherto few reports on asymmetric plaque burden in
22 A β mouse models due to the logistic difficulty of conducting onerous histological analysis
23 of both hemispheres for sufficient numbers of animals. We performed a meta-analysis
24 of the most recent 56 papers from journals with impact factor > 4 published in the
25 interval 2016 to 2019 with the key words “amyloid, mouse, model, AD”. 38% (21/56) of
26 these papers provided detailed information about use of different hemispheres for

1 histology and biochemistry. 81% among those (17/21) assigned a specific hemisphere to
2 a given modality, whereas only 19% (4/21) performed randomization of hemispheres to
3 different modalities. Most of the remaining 35 papers likewise split hemispheres to
4 different modalities, but without detailed information about the selection process.
5 Immunohistochemistry with A β antibodies like 6E10 was most frequently used to assess
6 fibrillar plaques *in vitro*, whereas other studies used histological staining with methoxy-
7 X04 or thioflavin S (14,25). These studies generally reported
8 immunohistochemistry/histology findings for A β quantification from a few representative
9 brain slices of a single hemisphere, whereas the other hemisphere was typically
10 reserved for biochemical assays such as Enzyme-linked Immunosorbent Assay or
11 western blotting, which are not compatible with tissue fixation. Therefore, evaluation of
12 intra-animal asymmetry *in vitro* was not feasible due to allocation of the hemispheres for
13 different kinds of analyses. In summary, potential asymmetries of fibrillar plaque burden
14 were only sparsely considered in published papers during the recent years.

15 Contrary to the case *in vitro*, A β -PET allows convenient quantification of amyloid
16 pathology in both whole hemispheres, with the caveat that the PET method has inherent
17 limitations in spatial resolution (26,27). Therefore, PET quantification of small brain
18 areas can be challenging, although asymmetry assessment A β plaque burden in large
19 forebrain regions is a rather robust measure. Thus, conducting non-invasive PET
20 examination prior to assignment of hemispheres to different terminal biochemical or
21 histological experiments could help to identify and adjust for relevant asymmetries of
22 plaque burden. This should encourage the combined use of PET together with
23 immuno(histochemistry) and biochemistry read outs.

24 Another focus of our study was to investigate the relationship between lateralized
25 A β deposition and microglial activation. Previous studies of our laboratory have already
26 shown close correlations between fibrillar amyloidosis and TSPO expression in

1 APP/PS1, PS2APP, APP-SL70 and *App*^{NL-G-F} mice (3,4,10,16). Although we
2 acknowledge that it was anticipated from these earlier findings, we now show for the first
3 time that microglial activation occurs concomitantly in the hemisphere ipsilateral with
4 predominant fibrillar amyloidosis. This association further strengthens the hypothesis
5 that initial fibrillar A β accumulation triggers neuroinflammation mediated by activated
6 microglia (28). Another recently published study has also demonstrated a link between
7 amyloidosis and neuroinflammation based on comparative profiling of cortical gene
8 expression in AD patients and an A β mouse model (29). Comparisons of gene
9 expression between hemispheres of mice with asymmetric amyloidosis could give new
10 insights into the molecular pathways and causal mechanisms underlying asymmetry in
11 AD. PET screening could guide the selection for detailed study of mice with strong
12 asymmetries.

13

14 **CONCLUSION**

15 Nearly a third of A β mice show distinct left- or right-asymmetry in the deposition
16 of cerebral amyloid. This phenomenon is neglected in the majority of current studies in
17 A β mice and calls for consideration in the planning and design of preclinical trials,
18 especially when single hemispheres are investigated by methods *ex vivo*. The lack of
19 age-dependency on asymmetric A β distribution implies that genetic factors underlie the
20 development of lateralized amyloidosis in AD model mice. There is a clear association
21 between asymmetries of glial activation and fibrillar amyloidosis in all A β mouse models
22 investigated in this study, further strengthening the hypothesis that neuroinflammatory
23 response to fibrillar A β contribute to the development of pathology in these mice.

24

1 **DISCLOSURE**

2 C.H. collaborates with Denali Therapeutics, participated on one advisory board
3 meeting of Biogen, and received a speaker honorarium from Novartis and Roche. C.H. is
4 chief advisor of ISAR Bioscience. P.B., A.R. and M.B. received speaking honoraria from
5 Life Molecular Imaging and GE healthcare. M.B. is an advisor of Life Molecular Imaging.
6 No other potential conflicts of interest relevant to this article exist.

7

8 **ACKNOWLEDGEMENTS**

9 C.H. is supported by the Koselleck Project HA1737/16-1 of the DFG, the
10 Helmholtz-Gemeinschaft (Zukunftsthema "Immunology and Inflammation" (ZT-0027)) and
11 the Cure Alzheimer's fund. The work was supported by the Deutsche
12 Forschungsgemeinschaft (M.B. and A.R. BR4580/1-1&RO5194/1-1). The APPPS1
13 colony was established from a breeding pair kindly provided by M. Jucker (Hertie-
14 Institute for Clinical Brain Research, University of Tübingen and DZNE-Tübingen).
15 APP^{swe}, PS2APP and APP-SL70 mice were provided by Hoffmann-La Roche. *APP^{NL-G-}*
16 *F* mice were provided by RIKEN BRC through the National Bio-Resource Project of the
17 MEXT, Japan. GE Healthcare made GE-180 cassettes available through an early-
18 access model.

19

1 **KEY POINTS**

2 QUESTION: Do amyloid mouse models have asymmetric plaque distribution and asymmetric
3 neuroinflammation?

4

5 PERTINENT FINDINGS: Asymmetry in these amyloid mouse models is frequent and statistically
6 relevant for planning of observational and interventional trials in these mice. Moreover,
7 asymmetries of fibrillar plaque burden and glial activation are positively correlated.

8

9 TRANSLATIONAL IMPLICATIONS: Lateralized distribution of fibrillar plaques is insufficiently
10 considered in experimental studies with amyloid mouse models and a potential confounder in
11 preclinical phases of drug development.

12

1 **REFERENCES**

2 **1.** Ziegler-Graham K, Brookmeyer R, Johnson E, Arrighi HM. Worldwide
3 variation in the doubling time of Alzheimer's disease incidence rates. *Alzheimers*
4 *Dement.* 2008;4:316-323.

5

6 **2.** Heneka MT, Carson MJ, El Khoury J, et al. Neuroinflammation in
7 Alzheimer's disease. *Lancet Neurol.* 2015;14:388-405.

8

9 **3.** Sacher C, Blume T, Beyer L, et al. Longitudinal PET Monitoring of
10 Amyloidosis and Microglial Activation in a Second-Generation Amyloid-beta
11 Mouse Model. *J Nucl Med.* 2019;60:1787-1793.

12

13 **4.** Brendel M, Probst F, Jaworska A, et al. Glial Activation and Glucose
14 Metabolism in a Transgenic Amyloid Mouse Model: A Triple-Tracer PET Study. *J*
15 *Nucl Med.* 2016;57:954-960.

16

17 **5.** Sasaguri H, Nilsson P, Hashimoto S, et al. APP mouse models for
18 Alzheimer's disease preclinical studies. *The EMBO Journal.* 2017;36:2473-2487.

19

20 **6.** Ossenkoppele R, Schonhaut DR, Scholl M, et al. Tau PET patterns mirror
21 clinical and neuroanatomical variability in Alzheimer's disease. *Brain.*
22 2016;139:1551-1567.

23

- 1 **7.** Tetzloff KA, Graff-Radford J, Martin PR, et al. Regional Distribution,
2 Asymmetry, and Clinical Correlates of Tau Uptake on [18F]AV-1451 PET in
3 Atypical Alzheimer's Disease. *J Alzheimers Dis.* 2018;62:1713-1724.
4
- 5 **8.** Frings L, Hellwig S, Spehl TS, et al. Asymmetries of amyloid-beta burden
6 and neuronal dysfunction are positively correlated in Alzheimer's disease. *Brain.*
7 2015;138:3089-3099.
8
- 9 **9.** Radde R, Bolmont T, Kaeser SA, et al. Abeta42-driven cerebral
10 amyloidosis in transgenic mice reveals early and robust pathology. *EMBO Rep.*
11 2006;7:940-946.
12
- 13 **10.** Parhizkar S, Arzberger T, Brendel M, et al. Loss of TREM2 function
14 increases amyloid seeding but reduces plaque-associated ApoE. *Nat Neurosci.*
15 2019;22:191-204.
16
- 17 **11.** Richards JG, Higgins GA, Ouagazzal AM, et al. PS2APP transgenic mice,
18 coexpressing hPS2mut and hAPPswe, show age-related cognitive deficits
19 associated with discrete brain amyloid deposition and inflammation. *J Neurosci.*
20 2003;23:8989-9003.
21

- 1 **12.** Ozmen L, Albientz A, Czech C, Jacobsen H. Expression of transgenic
2 APP mRNA is the key determinant for beta-amyloid deposition in PS2APP
3 transgenic mice. *Neurodegener Dis.* 2009;6:29-36.
4
- 5 **13.** Brendel M, Jaworska A, Overhoff F, et al. Efficacy of chronic BACE1
6 inhibition in PS2APP mice depends on the regional Abeta deposition rate and
7 plaque burden at treatment initiation. *Theranostics.* 2018;8:4957-4968.
8
- 9 **14.** Brendel M, Kleinberger G, Probst F, et al. Increase of TREM2 during
10 Aging of an Alzheimer's Disease Mouse Model Is Paralleled by Microglial
11 Activation and Amyloidosis. *Front Aging Neurosci.* 2017;9:8.
12
- 13 **15.** Blanchard V, Moussaoui S, Czech C, et al. Time sequence of maturation
14 of dystrophic neurites associated with Abeta deposits in APP/PS1 transgenic
15 mice. *Exp Neurol.* 2003;184:247-263.
16
- 17 **16.** Blume T, Focke C, Peters F, et al. Microglial response to increasing
18 amyloid load saturates with aging: a longitudinal dual tracer in vivo muPET-study.
19 *J Neuroinflammation.* 2018;15:307.
20
- 21 **17.** Masuda A, Kobayashi Y, Kogo N, Saito T, Saido TC, Itohara S. Cognitive
22 deficits in single App knock-in mouse models. *Neurobiol Learn Mem.*
23 2016;135:73-82.

1

2 **18.** Saito T, Matsuba Y, Mihira N, et al. Single App knock-in mouse models of
3 Alzheimer's disease. *Nat Neurosci.* 2014;17:661-663.

4

5 **19.** Rominger A, Brendel M, Burgold S, et al. Longitudinal assessment of
6 cerebral beta-amyloid deposition in mice overexpressing Swedish mutant beta-
7 amyloid precursor protein using 18F-florbetaben PET. *J Nucl Med.*
8 2013;54:1127-1134.

9

10 **20.** Brendel M, Jaworska A, Herms J, et al. Amyloid-PET predicts inhibition of
11 de novo plaque formation upon chronic gamma-secretase modulator treatment.
12 *Mol Psychiatry.* 2015;20:1179-1187.

13

14 **21.** Overhoff F, Brendel M, Jaworska A, et al. Automated Spatial Brain
15 Normalization and Hindbrain White Matter Reference Tissue Give Improved
16 [(18)F]-Florbetaben PET Quantitation in Alzheimer's Model Mice. *Front Neurosci.*
17 2016;10:45.

18

19 **22.** Raji CA, Becker JT, Tsopoulos ND, et al. Characterizing regional
20 correlation, laterality and symmetry of amyloid deposition in mild cognitive
21 impairment and Alzheimer's disease with Pittsburgh Compound B. *J Neurosci*
22 *Methods.* 2008;172:277-282.

23

- 1 **23.** Manook A, Yousefi BH, Willuweit A, et al. Small-animal PET imaging of
2 amyloid-beta plaques with [11C]PiB and its multi-modal validation in an APP/PS1
3 mouse model of Alzheimer's disease. *PLoS One*. 2012;7:e31310.
4
- 5 **24.** Brendel M, Jaworska A, Griessinger E, et al. Cross-sectional comparison
6 of small animal [18F]-florbetaben amyloid-PET between transgenic AD mouse
7 models. *PLoS One*. 2015;10:e0116678.
8
- 9 **25.** Cho SM, Lee S, Yang SH, et al. Age-dependent inverse correlations in
10 CSF and plasma amyloid-beta(1-42) concentrations prior to amyloid plaque
11 deposition in the brain of 3xTg-AD mice. *Sci Rep*. 2016;6:20185.
12
- 13 **26.** Visser EP, Disselhorst JA, Brom M, et al. Spatial resolution and sensitivity
14 of the Inveon small-animal PET scanner. *J Nucl Med*. 2009;50:139-147.
15
- 16 **27.** Huisman MC, Reder S, Weber AW, Ziegler SI, Schwaiger M. Performance
17 evaluation of the Philips MOSAIC small animal PET scanner. *Eur J Nucl Med Mol*
18 *Imaging*. 2007;34:532-540.
19
- 20 **28.** Monasor LS, Müller SA, Colombo A, et al. Fibrillar A β triggers microglial
21 proteome alterations and dysfunction in Alzheimer mouse models. *bioRxiv*.
22 2019:861146.
23

1 **29.** Castillo E, Leon J, Mazzei G, et al. Comparative profiling of cortical gene
2 expression in Alzheimer's disease patients and mouse models demonstrates a
3 link between amyloidosis and neuroinflammation. *Sci Rep.* 2017;7:17762.

4

5

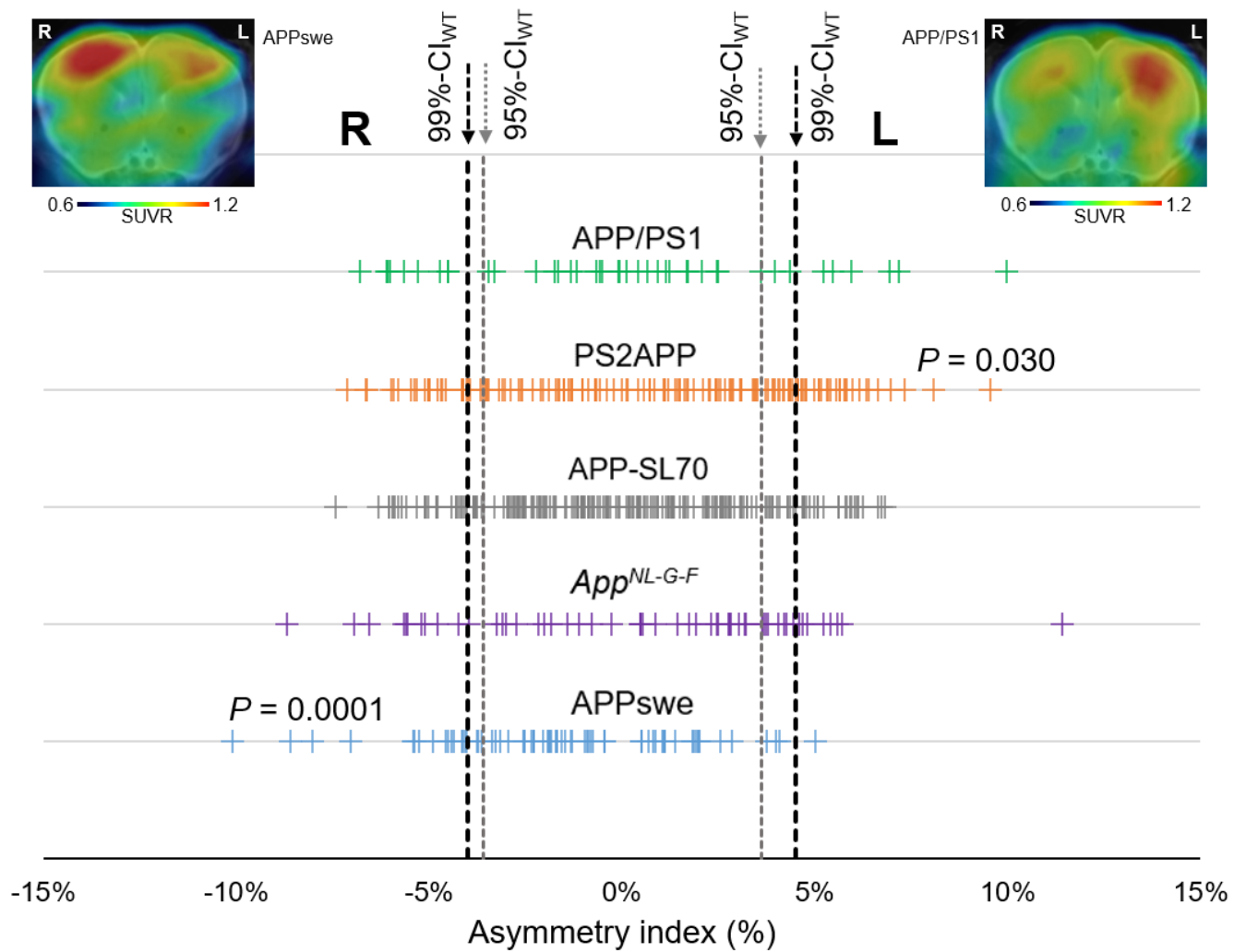


Figure 1 – Asymmetry of plaque distribution in amyloid mouse models. Forrest plot shows AI for a total of 523 amyloid PET scans in APP/PS1, PS2APP, APP-SL70, APP^{swe} and *App*^{NL-G-F} mice. Lateralized plaque distributions were compared by a Chi-square test to test for left or right predominance in each mouse model. Representative PET SUVR-images show exemplary mice with right (APP^{swe}) and left (APP/PS1) asymmetry.

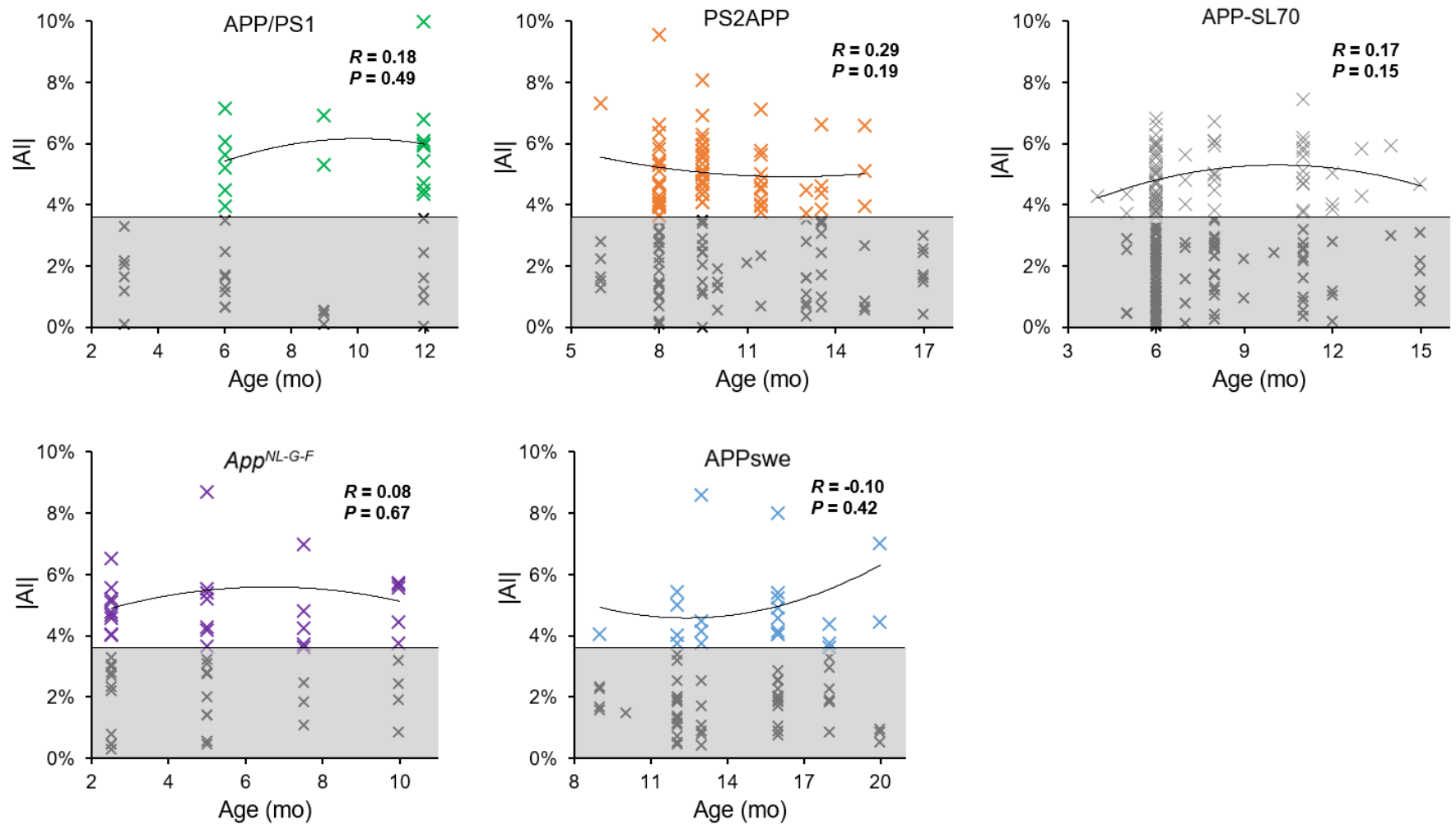


Figure 2 – Age dependency of asymmetric amyloid deposition. Asymmetry ($|AI|$) is shown as a function of age for APP/PS1, PS2APP, APP-SL70, APP^{swe} and *App*^{NL-G-F} mice. Datapoints with significant asymmetric ¹⁸F-FBB uptake ($|AI| > 95\%CI_{WT}$; light area) indicate no relevant dependency on asymmetric plaque distribution on age in any of the mouse models. Values with symmetric distribution (grey area) were excluded from the correlation analysis.

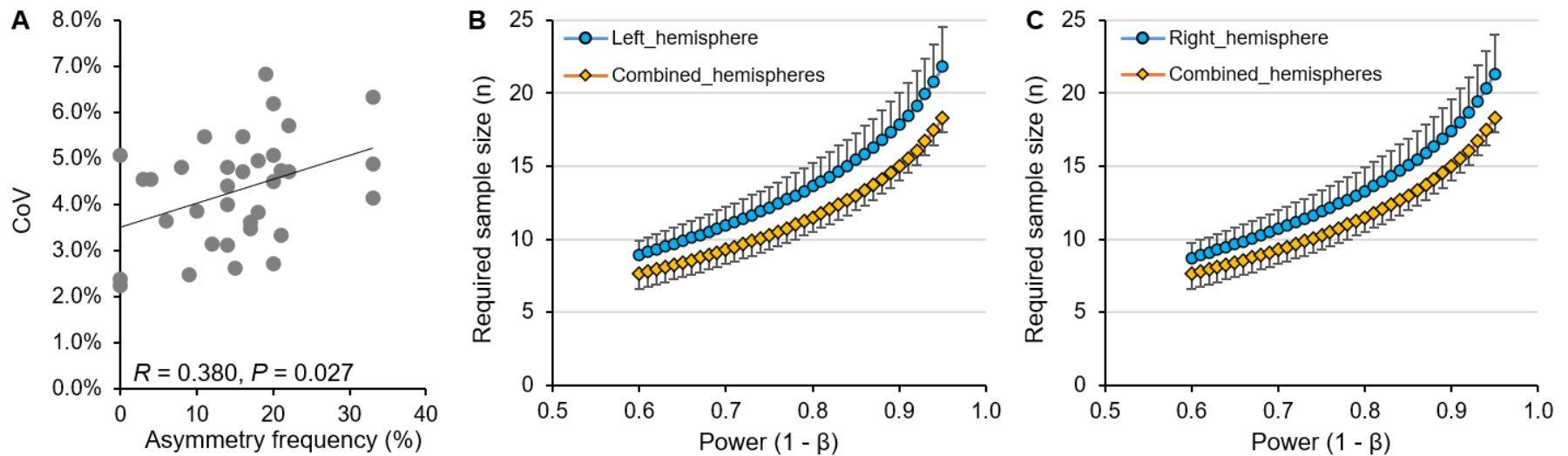


Figure 3 – Statistical relevance of asymmetric plaque distribution in amyloid mouse models. (A) Association of higher coefficients of variation (CoV) in SUVR with higher frequency of asymmetry in age related groups of amyloid mouse models (see supplemental Table 1). (B, C) Required sample sizes as a function of power in comparison of analyses in single hemispheres and combined hemispheres (given effect of 5%, $\alpha=0.05$, hypothetical 2-sided t-test of independent measures).

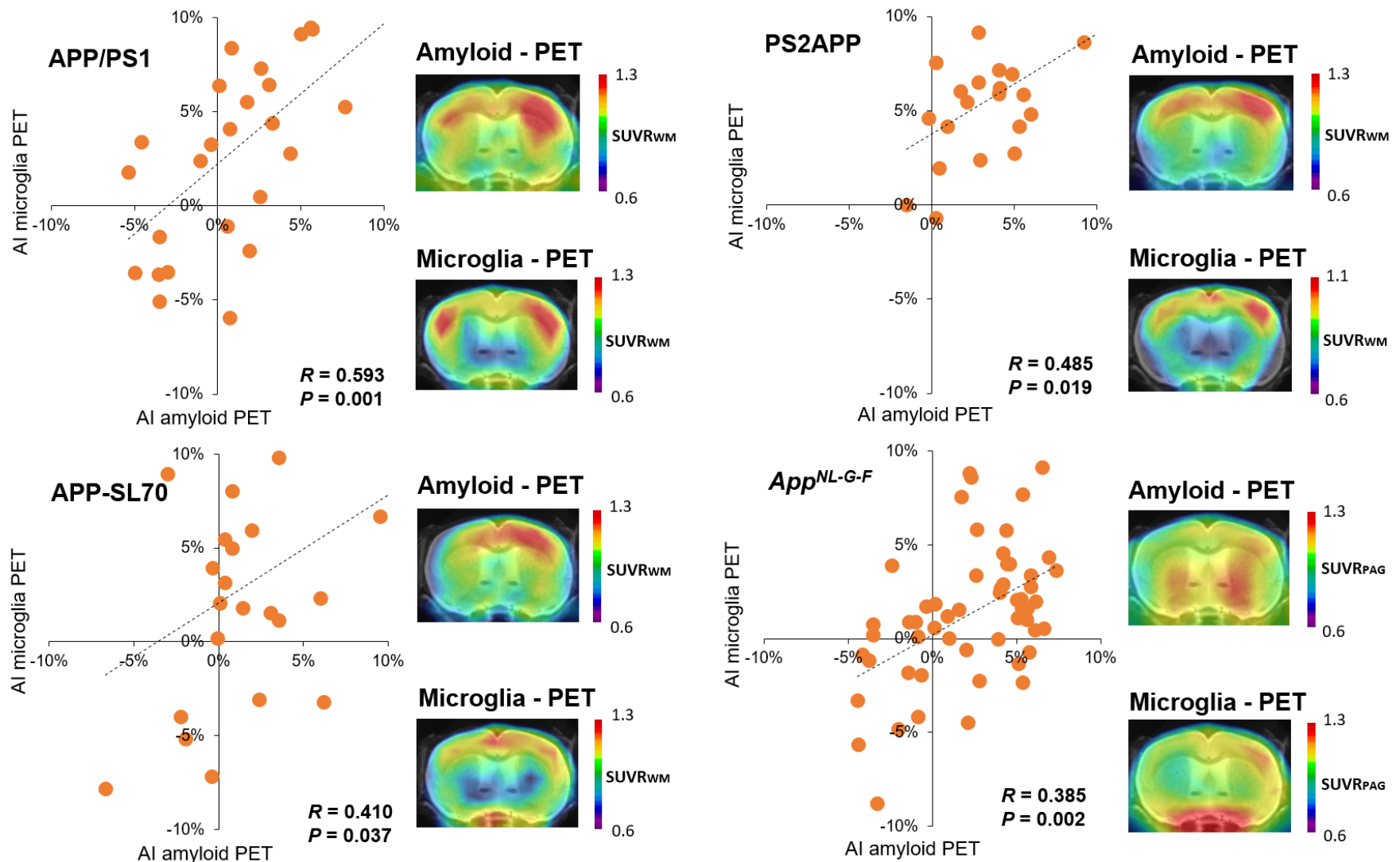


Figure 4 - Association between lateralized amyloid deposition and microglia activation. Correlations between AIs of amyloid and microglia PET in APP/PS1, PS2APP, APP-SL70 and *App^{NL-G-F}* mice show congruent asymmetry of both biomarkers. *R* indicates Pearson's coefficients of correlation.

Group	Age (months)	Amyloid-PET									TSPO-PET
		n	Moderate asymmetry (>/< 95%-CI _{WT})				Strong asymmetry (>/< 99%-CI _{WT})				
			Left (n, % per subgroup)	Left (n, % per model)	Right (n, % per subgroup)	Right (n, % per model)	Left (n, % per subgroup)	Left (n, % per model)	Right (n, % per subgroup)	Right (n, % per model)	
APP/PS1	3	6	0 (0%)	20%	0 (0%)	22%	0 (0%)	15%	0 (0%)	22%	0
	6	14	3 (21%)		3 (21%)		2 (14%)		3 (21%)		14
	9	6	1 (16%)		1 (17%)		1 (17%)		1 (17%)		5
	12	15	4 (27%)		5 (33%)		3 (20%)		5 (33%)		8
PS2APP	6 - 8	55	15 (27%)	30%	12 (22%)	19%	10 (18%)	21%	9 (16%)	16%	13
	9 - 10	42	16 (38%)		9 (21%)		14 (33%)		9 (21%)		10
	11 - 14	36	12 (33%)		5 (14%)		7 (19%)		4 (11%)		0
	15 - 17	14	1 (7%)		2 (20%)		0 (0%)		2 (14%)		0
APP-SL70	4 - 6	130	21 (16%)	18%	20 (15%)	16%	12 (9%)	12%	16 (12%)	13%	0
	7 - 9	37	6 (16%)		6 (16%)		5 (14%)		5 (14%)		8
	10 - 12	31	8 (26%)		7 (23%)		6 (19%)		5 (16%)		10
	13 - 15	10	3 (30%)		1 (10%)		2 (20%)		1 (10%)		8
App ^{NL-G-F}	2.5	20	4 (20%)	29%	5 (25%)	20%	3 (15%)	10%	4 (20%)	18%	17
	5	17	4 (24%)		3 (18%)		1 (6%)		3 (18%)		15
	7.5	9	4 (44%)		2 (22%)		2 (22%)		2 (22%)		11
	10	9	4 (44%)		1 (11%)		2 (22%)		1 (11%)		12
APP ^{swe}	9 - 12	26	3 (12%)	6%	2 (8%)	26%	1 (4%)	2%	2 (8%)	22%	0
	13 - 16	30	1 (3%)		11 (37%)		0 (3%)		10 (33%)		0
	17 - 20	16	0 (0%)		6 (38%)		0 (0%)		4 (25%)		0
C57BL/6 (wild-type)	2.5 - 16	27									

Supplemental Table 1 – Overview of the animal cohorts studied by A β -PET and TSPO-PET and their frequency of asymmetry in A β -PET